Journal of Marine Science and Technology

Volume 20 | Issue 4 Article 6

STUDY ON THE SEISMIC BEHAVIOR OF SELF-ANCHORED SUSPENSION BRIDGES

Wen-Liang Qiu
School of Civil Engineering, Dalian University of Technology, Dalian City, Liaoning Province, China, P.R.C.

Chang-Huan Kou
Department of Civil Engineering, Chunghua University, Hsinchu City, Taiwan, R.O.C., chkou@chu.edu.tw

Chin-Sheng Kao
Department of Civil Engineering, Tamkang University, Tamsui, Taipei County, Taiwan, R.O.C.

Shih-Wei Ma
Department of Civil Engineering, Chunghua University, Hsinchu City, Taiwan, R.O.C.

Jiun Yang
School of Civil Engineering, Dalian University of Technology, Dalian City, Liaoning Province, China, P.R.C.

Journal of Marine Science and Technology, Vol. 20, No. 4, pp. 384-391 (2012)
DOI: 10.6119/JMST-011-0304-1

STUDY ON THE SEISMIC BEHAVIOR OF SELF-ANCHORED SUSPENSION BRIDGES

Wen-Liang Qiu[1], Chang-Huan Kou[2], Chin-Sheng Kao[3], Shih-Wei Ma[2], and Jiun Yang[1]

Key words: self-anchored suspension bridge, seismic behavior, ductility seismic response analysis, metal damper seismic response analysis.

ABSTRACT

The suspension bridge has a beautiful structural shape and an excellent spanning ability. The self-anchored suspension bridge has its main cables anchored directly on the two ends of the main girders, saving construction costs and time incurred during the anchorage construction of an earth-anchored suspension bridge. However, the feasibility of a self-anchored suspension bridge in a strong earthquake zone and the use of dampers to reduce seismic responses have yet to be fully investigated.

Using the Yellow-River Road Bridge in Mainland as an example, this study sets out to analyze and investigate a series of seismic responses of a self-anchored suspension bridge, with the purpose of understanding its seismic responses in a strong earthquake zone and the effectiveness of metal dampers in reducing the seismic response. In this paper, in addition to performing a linearly elastic seismic analysis, the ductility seismic response was also analyzed. Additionally, metal dampers were installed at the joints of main girders and towers so that the energy damping effect can be investigated. The results of this research will be useful to the academic research community and for practical engineering applications.

I. INTRODUCTION

The suspension bridge is a flexural bridge structure composed of main cables, hangers, bridge towers and main girders. Due to the beautiful structural shape and its spanning capability, the suspension bridge is often seen as a landmark structure crossing a river. Because its main cables are anchored directly on the two ends of the main girders, the self-anchored suspension bridge can save much costs and time spent on constructing the anchorages of an earth-anchored suspension bridge. In addition, the axial compressive forces exerted by the main cables on the main girders may be used as prestressed forces for the girders which can increase the bending resistance capacity of the reinforced concrete main girders. Thus, the self-anchored suspension bridge is an economical suspension bridge.

Due to the differences in anchorage, the seismic response of a self-anchored suspension bridge is different from that of an earth-anchored suspension bridge. It has its own characteristics. Because the main cables are anchored on the two ends of the main girders, the anchors move together with the girders and the tops of the towers also move with the main girders due to the linking of the cables, which makes of the self-anchored suspension bridge to be a longitudinal floating system. Under the longitudinal seismic force, the displacements of the main girders and the top of the towers, and the bending moments at the tower bottoms are all very large. Thus, the most important part of the seismic design for this type of bridge is to control the forces and displacements of the bridge by use of damping devices.

The early constructed self-anchored suspension bridges with short span all use steel main girders [7], so the seismic responses do not control the bridge design and few studies on the seismic response of self-anchored suspension bridges were carried out. However, with some long-span self-anchored suspension bridges building in recent years, seismic action often controls the forces and displacements of the design especially for self-anchored suspension bridges with reinforced concrete main girders. Investigators have started to pay attention to the seismic resistance of the self-anchored suspension bridge. Liu *et al.* [4, 5] derived the governing differential equations for determining the natural vibration of a self-anchored suspension bridge. He considered the dynamic seismic space effect and applied the pseudo-exciting method to study the longitudinal seismic response of a self-anchored suspension bridge subjected to random excitations at various points along the bridge. On the other hand, Yang *et al.* [8] performed a nonlin-

Paper submitted 03/12/10; revised 01/14/11; accepted 03/04/11. Author for correspondence: Chang-Huan Kou (e-mail: chkou@chu.edu.tw).
[1] *School of Civil Engineering, Dalian University of Technology, Dalian City, Liaoning Province, China, P.R.C.*
[2] *Department of Civil Engineering, Chunghua University, Hsinchu City, Taiwan, R.O.C.*
[3] *Department of Civil Engineering, Tamkang University, Tamsui, Taipei County, Taiwan, R.O.C.*

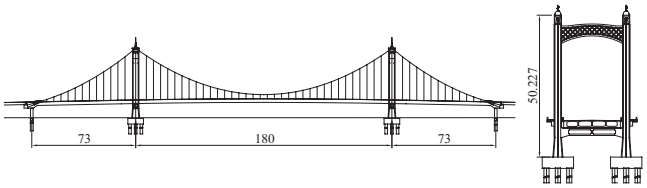

Fig. 1. The layout of the main Yellow River Road Bridge in Mainland (unit: m).

ear time-history analysis and investigated the seismic characteristics of a single tower self-anchored suspension bridge. McDaniel *et al*. [6] used inelastic tower links to educe the seismic responses of tower of the new San Francisco-Oakland Bay Bridge East Span self-anchored suspension bridge with global seismic time history analyses. Fang *et al*. [1] studied the energy and vibration reduction designs by installing viscous damper and lead extrusion damper between the main girder and tower while Jiang *et al.* [3] performed a parametric analysis for the self-anchored suspension bridge based on dissipation due to elastic collision and viscous damper between the tower and girder. Gao *et al*. [2] studied the optimization of seismic resistance design of the tower and the location of dampers for a self-anchored suspension bridge.

This paper presents a nonlinear time-history method to investigate the seismic response of a self-anchored suspension bridge, considering the geometric nonlinearity of the structure and the material nonlinearity of the tower. Also investigated herein is the damping effect of the metal damper which is stable and easily maintained.

II. ANALYSIS OF BRIDGE STRUCTURE AND ITS SEISMIC RESPONSE

2. The Bridge Structure

The Yellow River Road Bridge is a three-span self-anchored suspension bridge. The main span is 180 m and the side spans are 73 m each with a total length of 326 m. The main cables have a rise-span ratio of 1/5.5. The general layout of the bridge is shown in Fig. 1. Longitudinal movable supports are used under the main bridge at the towers and side piers. Transverse displacement-limiting bearings are installed at the main piers and the gaps between the bearings and the main girders are 1.0 cm. The main girder is a pre-stressed concrete box girder with two pre-stressed main cable anchorage at the both ends. The tower has the shape of a gate and the column of the tower has a solid cross section of 3.5 m × 5.5 m at the bottom of tower, gradually changed to 2.5 m × 4.5 m just under the girder, and 2.5 m × 4.5 m for the upper part of the column. Pile groups are used for the foundations of the towers. There are nine 1.8 m-diameter drilled piles underneath each column. The bridge has two main cables and each cable is made of 4699 paralleled, 5 mm in diameter, high strength galvanized steel wires. The hangers are also made of parallel high strength galvanized steel wires.

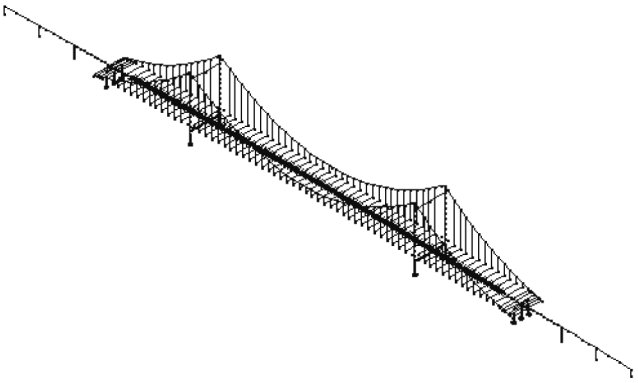

Fig. 2. The finite element model of the Yellow River Road Bridge.

2. Method of Analysis

The ANSYS finite element software and a space element model are used to investigate the dynamic characteristics and seismic response of the Yellow River Road Bridge. In the seismic response analysis, time-history analysis was conducted to consider the geometrical and material nonlinearity of the structure. The finite element model is shown in Fig. 2. Beam element was used for the tower columns, the piers, the piles, the main girders and the cross beams. The foundations were simplified as a spring models. The main cables and hangers were modeled as a truss element. The analysis considered the effects of large displacement in the main cables and hangers and the rigidity at initial loading. In ANSYS, the 3D elastic Beam 4 element was used to model the tower and the bridge deck system (main girders and cross beams); while truss element Link 10 was used to model the main cables and hangers.

3. Seismic Wave Used for Analysis and Artificial Seismic Waves

For the seismic response time-history structural analysis, the seismic wave used in the analysis can either be an actual seismic wave with some adjustments or an artificial seismic wave.

The methods for generating the artificial seismic waves include code response spectrum simulated by the trigonometric series, directly simulated code response spectrum, superposition method in the time domain to simulate the code response spectrum, semi-empirical iteration to simulate the code response spectrum, an artificial seismic wave based on the power spectrum, and the ARMA model.

The following equation based on Kaul's relation between the response spectrum and the power spectrum is adopted to obtain the artificial seismic wave by simulating the code response spectrum:

$$S_x(\omega_k) = \frac{2\xi}{\pi\omega_k}\left[S_a^T(\omega_k)\right]^2 \Bigg/ \left[-2\ln\left(-\frac{\pi}{\omega_k T_d}\ln p\right)\right] \quad (1)$$

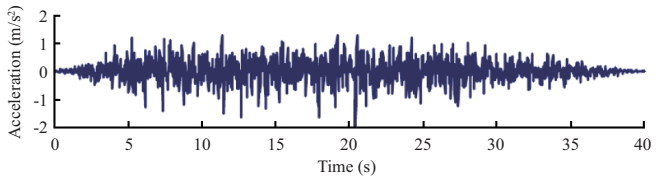

Fig. 3. Artificial seismic wave.

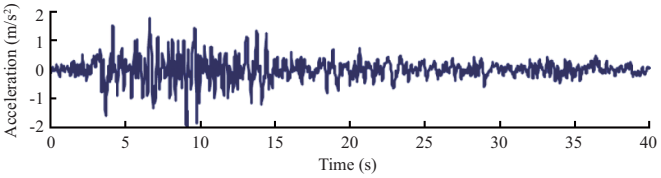

Fig. 4. Taft seismic wave.

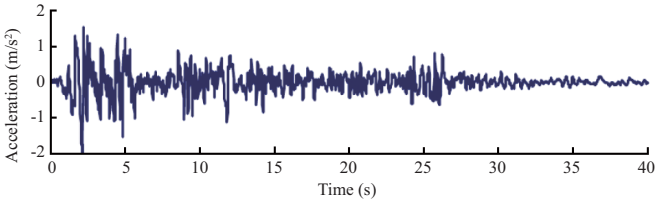

Fig. 5. El Centro seismic wave

where $S_a^T(\omega_k)$ is a given code response spectrum, ξ is the damping ratio, T_d is the time duration of the seismic wave; and p is the probability of not exceeding the response spectrum value. (Usually $p \geq 0.85$)

Calculation using the following two equations led to a stable Gaussian process $A(t)$ with a zero mean value:

$$A(t) = \sum_{k=1}^{N} C_k \cos(\omega_k t + \varphi_k) \tag{2}$$

$$\begin{cases} C_k = \left[4S_x(\omega_k)\Delta\omega\right]^{1/2} \\ \Delta\omega = (\omega_u - \omega_l)/N \\ \omega_K = \omega_L + (k - 1/2)\Delta\omega \end{cases} \tag{3}$$

where ω_k and C_k are the frequency and amplitude of the kth Fourier component respectively; φ_k is the initial phase angle with the probability function of an uniform distribution between $(0, 2\pi)$, ω_u and ω_l are the upper and lower bounds in the positive ω region respectively; and N is a positive number dividing (ω_u, ω_l) into N number of equal divisions.

The nonstationary Gaussian process was calculated by

$$x(t) = f(t)A(t) \tag{4}$$

where the envelope function $f(t)$ is:

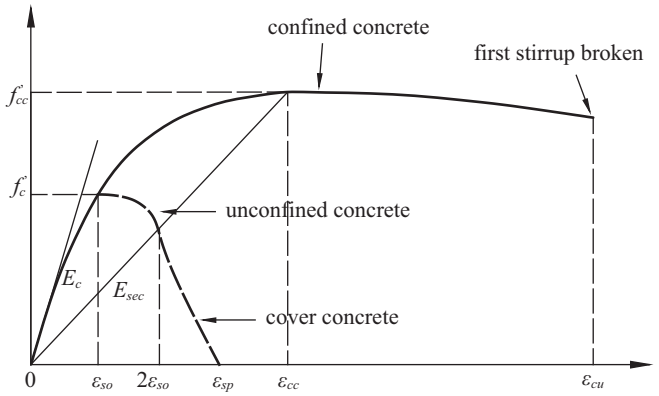

Fig. 6. Stress-strain relationship curve of confined concrete.

$$f(t) = \begin{cases} (t/t_1)^2 & 0 \leq t \leq t_1 \\ 1 & t_1 \leq t \leq t_2 \\ e^{-c(t-t_2)} & t_2 \leq t \leq t_3 \end{cases} \tag{5}$$

where c is the attenuation constant with value between 0.1~1.0, t_1, t_2 and t_3 are constants related to the intensity of earthquake and soil condition.

The artificial seismic wave created from the above procedure is shown in Fig. 3. This artificial seismic wave is generated based on the design response spectrum of the Seismic Design Specification for Highway Bridges of China. The site classification belongs to the II category, which is consistent with the analyzed Huanghe Road Bridge. The upper limit adopted by this research during the generation of artificial seismic waves is 50 Hz, the lower limit 0.05 Hz, and the interval 0.025 Hz. In addition to using this artificial seismic wave in the time-history analysis, two frequently used seismic acceleration records (Taft and El Centro seismic wave) were used as shown in Figs. 4 and 5. The acceleration peak values were all adjusted to 0.2 g for consideration of frequently occurred earthquake.

4. The Material Nonlinearity of Reinforced Concrete

1) Constitutive Relation for Concrete

The Mander stress-strain model was used for confined concrete in this paper, as shown in Fig. 6. The equations are:

$$f_c = \frac{f'_{cc} x r}{r - 1 + x^r} \tag{6}$$

$$x = \varepsilon_c / \varepsilon_{cc} \tag{7}$$

$$\varepsilon_{cc} = \left[5\left(\frac{f'_{cc}}{f'_c} - 1\right) + 1\right]\varepsilon_{co} \tag{8}$$

where f'_{cc} is the peak compressive strength of confined con-

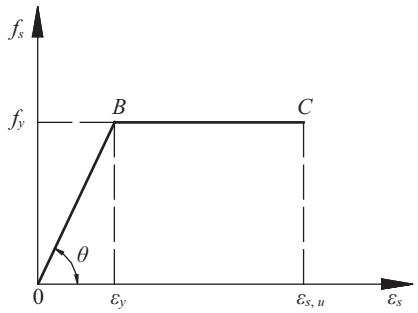

Fig. 7. Stress-strain relationship curve of reinforcing steel.

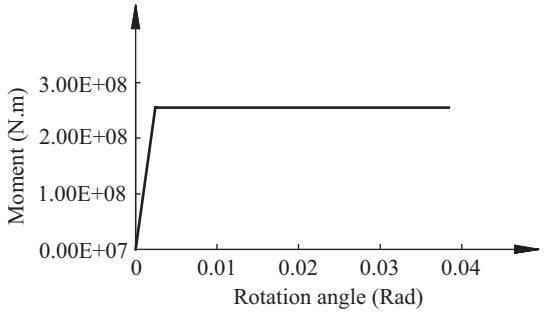

Fig. 8. Moment-rotation angle relationship curve of plastic hinge.

crete, ε_c is the compressive strain of concrete; ε_{cc} is the compressive strain corresponding to f'_{cc}, f'_c and ε_{co} are the non-confined compressive strength of concrete and its corresponding compressive strain respectively (usually $\varepsilon_{co} = 0.002$).

$$r = E_c / (E_c - E_{\text{sec}}) \tag{9}$$

$$E_c = 5000\sqrt{f'_c} \text{ (Unit for } f'_c \text{ and } E_c \text{ is MPa)} \tag{10}$$

$$E_{\text{sec}} = f'_{cc} / \varepsilon_{cc} \tag{11}$$

2) Constitutive Relation for Reinforcing Steel

The stress-strain relation for reinforcing steel used in this paper was a perfectly elasto-plastic model with a bi-linear stress-strain curve as shown in Fig. 7. Its equations are:

$$\text{When } \varepsilon_s \le \varepsilon_y, \sigma_s = E_s \varepsilon_s \ (E = \frac{f_y}{\varepsilon_y}), \tag{12}$$

$$\text{When } \varepsilon_y \le \varepsilon_s \le \varepsilon_{s,h}, \sigma_s = f_y, \tag{13}$$

3) A Plastic Hinge Method for the Reinforced Concrete Tower

Based on elastic analysis, the bottom of the tower of Yellow River Road Bridge is the first part entering its elasto-plastic stage under longitudinal earthquake. Therefore, in the ductility analysis, the plastic hinge was located at the bottom of tower. The ductility capacity of the plastic hinge was very important in the assessment of the seismic resistance of the structure through seismic energy absorption and ductility index. The ductility capacity of a plastic hinge was determined by the length of the hinge and by the moment-curvature relation of the reinforced concrete component.

The Eurocode 8 was used to determine the length of the plastic hinge. The length of the plastic hinge, L_p is

$$L_P = 0.08L + 0.022 d_s f_y \tag{14}$$

$$\text{or } L_P = (0.4/0.6)H \tag{15}$$

where L is the height of the pier, H is the height of the cross section, d_s and f_y are the diameter of the longitudinal reinforcing steel and yield stress respectively. Based on the actual dimensions of the tower cross section of Yellow River Road Bridge and the reinforcing steel used, the length of the plastic hinge was calculated to be $L_P = 3.33$ *m*.

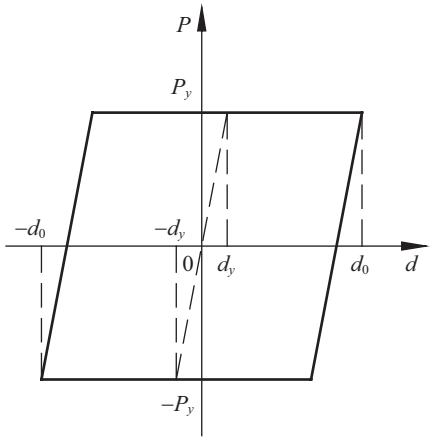

Fig. 9. Moment-rotation angle relationship curve of plastic hinge.

Using the aforementioned constitutive relations for concrete and reinforcing steel, the Ucfyber software was used to calculate the moment-curvature relation at the bottom of the tower of Yellow River Road Bridge, which led to the relationship of moment and angular displacement at plastic hinge as shown in Fig. 8.

The ANSYS finite element software was used in this study to perform a ductility seismic response analysis of the Yellow River Road Bridge. The combin 39 spring element was used to simulate the plastic hinge.

4) Mechanical Model for Metal Damper

The most commonly used restoring force models for a metal damper include perfectly elasto-plastic model and bi-linear model. Here, the perfectly elasto-plastic model was used as shown in Fig. 9.

The initial elastic stiffness could be calculated from the equation below:

$$k_\varepsilon = P_y / d_y \tag{16}$$

Table 1. Summary of the natural frequency and vibration mode.

No	Frequency (Hz)	Vibration mode
1	0.22387	longitudinal floating mode of main girder
2	0.44796	first symmetrical vertical bending mode of main girder
3	0.56726	first unsymmetrical vertical bending mode of main girder
4	0.91140	symmetrical lateral bending mode of main girder
5	0.94816	second symmetrical vertical bending mode of main girder
6	0.95922	second unsymmetrical vertical bending mode of main girder

When displacement of the device exceeded d_y, the restoring force was P_y. The dissipated energy for each cycle, W_d was equal to the area of hysteresis loop between point (P_y, d_0) and point ($-P_y$, $-d_0$), i.e.:

$$W_d = 4P_y(d_0 - d_y)(d_0 > d_y) \tag{17}$$

$$\beta_\varepsilon = \frac{4P_y(d_0 - d_y)}{2\pi k_\varepsilon d_0^2} \tag{18}$$

III. ELASTIC SEISMIC RESPONSE ANALYSIS OF SELF-ANCHORED SUSPENSION BRIDGE

1. Dynamic Characteristics Analysis

In order to understand the dynamic characteristics and the regularities of seismic response of a self-anchored suspension bridge, the space element model of Fig. 2 was first used to calculate the dynamic properties of the Yellow River Road Bridge. The natural frequency and mode shape were obtained. Table 1 shows the first six modes of vibration. It can be seen from the natural frequency and mode shape that the first mode of the self-anchored suspension bridge was a longitudinal floating mode with a longer period. This mode directly affected the internal force and displacement of the bridge subjected to longitudinal seismic action.

2. Seismic Response Time-History Analysis

Referring to the measured damping ratio of 0.5%~1.5% for the two suspension bridges, i.e. Hu-men Bridge and Jiang-In Bridge, the damping ratio of the bridge studied in this paper was taken as 1%.

The analysis showed that when the bridge was subjected to a transverse seismic wave, the seismic response did not control the design of the bridge. However, when subjected to a longitudinal seismic wave, the seismic response was very noticeable, and the main responses were the longitudinal floating of main girder and longitudinal vibration of the tower. The response analysis results produced by the three seismic waves were quite different. The responses produced by the artificial seismic wave were larger than that produced by Taft seismic wave and El Centro seismic wave. So the following studies were all based on the artificial wave.

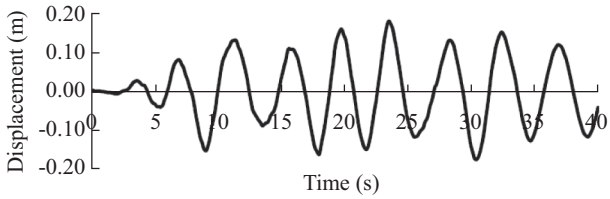

Fig. 10. Longitudinal displacement time-history response of the main girder under longitudinal excitation.

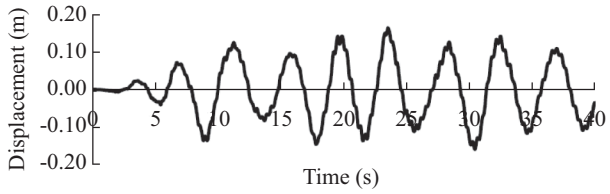

Fig. 11. Longitudinal displacement time-history response at tower top under longitudinal excitation.

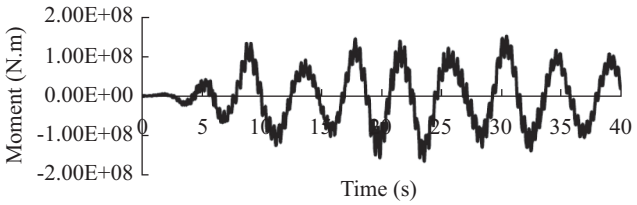

Fig. 12. Longitudinal bending moment time-history response at tower bottom under longitudinal excitation

Under the longitudinal excitation of artificial seismic wave, the maximum longitudinal displacement of the main girder was 0.183 m, the maximum longitudinal displacement at the tower top was 0.165 m, and the maximum bending moment along the longitudinal direction at the base of the tower was 1.65×10^8 N-m. At this point of time, the time histories of the longitudinal displacement of the girder, the displacement of the top of the tower, and the bending moment are shown in Figs. 10-12.

IV. DUCTILITY SEISMIC RESPONSE ANALYSIS OF SELF-ANCHORED SUSPENSION BRIDGE

1. Analysis Results of Ductility Seismic Response

The finite element model used in the ductility seismic response analysis is the same as that used in the elastic seismic response analysis. Nevertheless, since there was a plastic hinge at the tower base, the material nonlinearity was considered for the tower in the ductility analysis. In the time-history analysis, the effect of geometric nonlinearity was considered.

Table 2. Comparison of seismic response.

Seismic Analysis	Seismic intensity	Displacement of Girder (m)	Displacement at Tower Top (m)	Moment at Tower Bottom (N-m)
Elastic analysis	VII	0.183	0.165	1.65×10^8
Elastic analysis	VIII	0.464	0.421	4.22×10^8
Ductility analysis	VIII	0.620	0.599	2.55×10^8

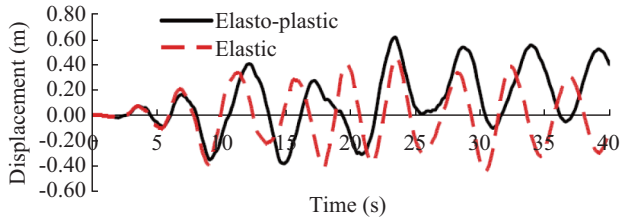

Fig. 13. Longitudinal displacement time-history response of the main girder under longitudinal excitation.

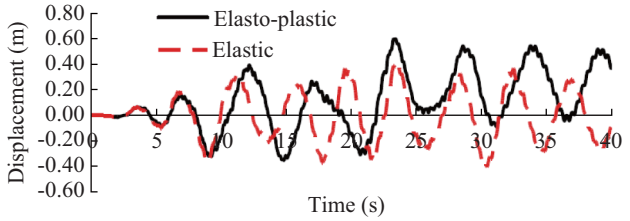

Fig. 14. Longitudinal displacement time-history response at tower top under longitudinal excitation.

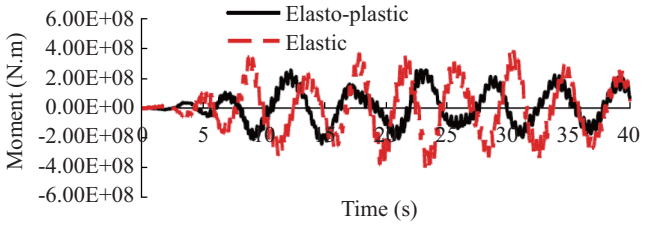

Fig. 15. Longitudinal bending moment time-history response of the plastic hinge under longitudinal excitation.

The artificial seismic wave was inputted into the model to perform ductility time-history analysis, and the peak value of the acceleration of seismic wave was adjusted to 0.51 g for consideration of rarely occurred earthquake. Under excitation of artificial longitudinal seismic wave, the maximum longitudinal displacement of the main girder was 0.620 m, the maximum longitudinal displacement at the tower top was 0.599 m, the maximum bending moment in the longitudinal direction of the plastic hinge at the tower bottom was 2.55×10^8 N-m, and the maximum angular displacement of the plastic hinge was 0.00789 rad. The seismic time-history responses of longitudinal displacement of the girder, the displacement of the tower top, the bending moment of the plastic hinge, and the angular displacement are shown in Figs. 13-16 and Table 2.

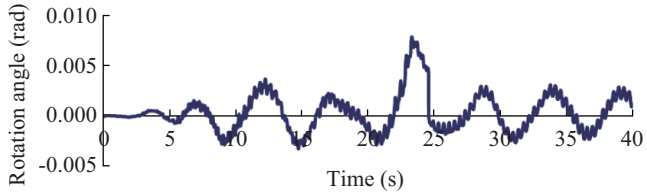

Fig. 16. Longitudinal rotation angle time-history response of the plastic hinge under longitudinal excitation.

The results of the elastic analysis are also shown in the same figures.

V. SEISMIC RESPONSE REDUCTION ANALYSIS OF SELF-ANCHORED SUSPENSION BRIDGE WITH METAL DAMPERS

Through the previous analysis, the Yellow River Road Bridge was found to have excessive displacement in the girder when subjected to seismic loading. Thus, a damping device was necessary to satisfy the safety requirement of the structure. Due to the advantages of using metal dampers, they were selected as the damping device for this bridge. The metal dampers were installed to connect the tower and the girder. Here, two metal dampers were installed for each tower. In total, four dampers were used for the bridge.

The metal dampers of this bridge satisfy the perfectly elasto-plastic model shown in Fig. 9. The choice of damper must satisfy the following requirement: the damper must be in the elastic stage under temperature loads and it must enter the plastic stage under seismic loads. Due to the hysteresis loop, energy was dissipated and d_y was taken to be 5 cm. For the rarely occurred earthquake, the displacement of the girder and the top of the towers were controlled. The displacement of the girder was controlled to within 15 cm to protect the expansion joints and to control bending moment of the bottom of the tower.

In the construction of a model for energy dissipation and seismic mitigation analysis, the metal damper was simulated by spring elements, i.e. four springs were placed along the longitudinal direction of the bridge. The mechanical model of the damper is shown in Fig. 7 where k_ε denotes the elastic stiffness. In the case of the rarely occurred artificial longitudinal seismic wave, different parameters were used in the calculation (P_y or k_ε), and the hysteresis loops of the metal dampers are shown in Fig. 17. The results of the calculation are shown in Table 3.

Table 3. Effects of metal damper with different k_e parameter.

Parameter of Damper k_e (N/m)	Displacement of The Girder (m)	Displacement at Tower Top (m)	Moment at Tower Bottom (N-m)
4.5×10^7	0.201	0.197	2.15×10^8
5.0×10^7	0.168	0.166	1.91×10^8
5.5×10^7	0.147	0.146	1.85×10^8
6.0×10^7	0.130	0.129	1.89×10^8
No damper	0.464	0.421	4.22×10^8

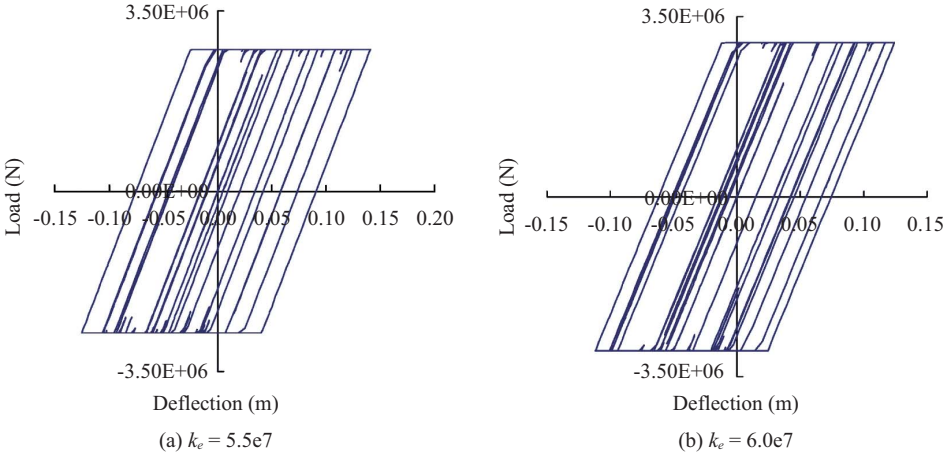

Fig. 17. Load-deflection relationship of metal damper.

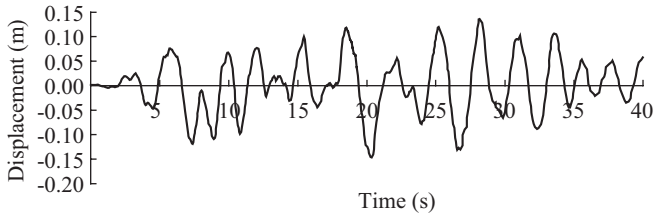

Fig. 18. Longitudinal displacement time-history response of the main girder under longitudinal excitation.

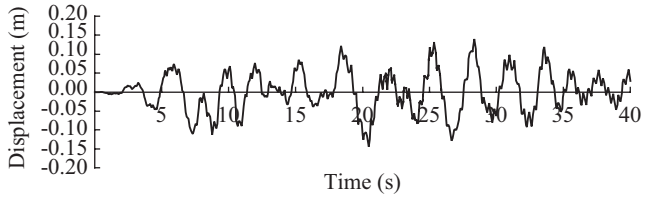

Fig. 19. Longitudinal displacement time-history response at tower top under longitudinal excitation.

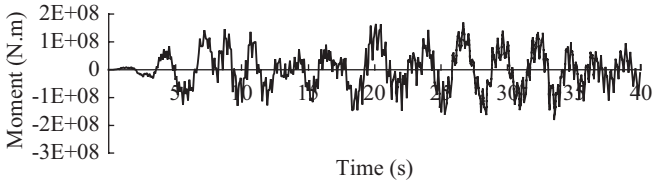

Fig. 20. Longitudinal bending moment time-history response at tower bottom under longitudinal excitation.

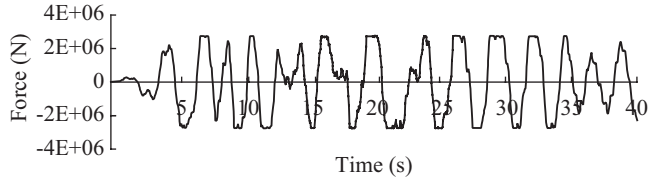

Fig. 21. Restoring force time-history response of the metal damper under longitudinal excitation.

It can be seen from the above analysis that the metal damper was quite sensitive to the choice of parameters. The metal damper was quite effective in the hysteretic energy dissipation and it could effectively reduce the longitudinal displacement of the main girder and the horizontal displacement at the tower top. Besides, it could effectively protect the structure and reduced the bending moment of the tower. For the rare earthquake of intensity VIII, when the damper parameter was $k_\varepsilon = 5.5 \times 10^7$ (N/m), the displacement of the main girder reduced from 0.464 m to 0.147 m, the displacement at the tower top reduced from 0.421 m to 0.146 m, and the bending moment at the tower bottom reduced from 4.22×10^8 N-m to 1.85×10^8 N-m. Time-histories for the displacement of the girder, the displacement at the tower top, the moment at the tower bottom and the restoring force for the damper are shown in Figs. 18-21.

VI. CONCLUSIONS

Using the Yellow River Road Bridge in China as an example, the present paper investigated the dynamic characteristics, elastic seismic response, ductility seismic response, and energy dissipation and seismic response reduction effect of the metal dampers for the self-anchored suspension bridge. The main conclusions are:

1. From the dynamic characteristics analysis, it was found that the self-anchored suspension bridge retains two specific features similar to the earth-anchored suspension bridge. One is the low mode has a longer period, the other is the concentration of vibration modes. Due to the free motion of the main girder along the longitudinal direction, the first vibration mode is longitudinal floating, which is similar to the cable-stayed bridge of the floating system. It is beneficial to the structural seismic response, but leads to large longitudinal displacement thus resulting in a seismic disaster of dropping girder or damaging expansion joints of the bridge.
2. Since earthquake is a random process, several seismic waves must be considered and compared in the seismic time-history analysis. In this paper, two recorded seismic waves and an artificial wave were used to analyze the time-history of the frequent earthquake. It can be deduced from the results that for the self-anchored suspension bridge with a longitudinal floating first mode, displacements are large for the main girders and the tower top, and the bending moment is large at the bottom of the tower.
3. Comparing with elastic response analysis for the Yellow River Road Bridge, the moment of the bottom of the tower was drastically reduced when using ductility analysis. Therefore, in the ductility design, the seismic resistance of a suspension bridge is greatly increased, while displacements of the main girder and the tower top are apparently increased. These factors should be carefully considered in the design.
4. After installation of the metal dampers along the longitudinal direction, longitudinal displacements of the girder and tower can be well controlled when subjected to the action of longitudinal earthquake, and bending moment of the bottom of the tower can also be reduced largely. Bridge components, such as expansion joints, were well protected and the girder was prevented from dropping.

REFERENCES

1. Fang, H., Liu, W. Q., and Wang, R. G., "Design method of energy-dissipating earthquake reduction along longitudinal direction of self-anchored suspension bridge," *Earthquake Engineering and Engineering Vibration*, Vol. 26, No. 3, pp. 222-225 (2006).
2. Gao, Y., Yuan, W. C., Zhou, M., and Cao, X. J., "Seismic analysis and design optimization of a self-anchored suspension bridge," *Lifeline Earthquake Engineering in a Multihazard Environment (TCLEE2009)*, ASCE, Oakland, California, United States, pp. 153-164 (2009).
3. Jiang, M., Qiu, W. L., and Yu, B. C., "Research on seismic response reduction of self-anchored suspension bridge," *Proceedings of the International symposium on Computational and Structural Engineering (CSE2009)*, Shanghai, China, pp. 209-216 (2009).
4. Liu, C. C., Zhang, Z., and Shi, L., "Analysis of longitudinal seismal response for self-anchored suspension bridges," *Journal of Wuhan University of Technology*, Vol. 26, No. 5, pp. 607-610 (2002).
5. Liu, C. C., Zhang, Z., Shi, L., and Du, P. J., "Theoretical study of vertical free vibrations of concrete self-anchored suspension bridges," *Engineering Mechanics*, Vol. 22, No. 4, pp. 126-130 (2005).
6. McDaniel, C. C. and Seible, F., "Influence of inelastic tower links on cable-supported bridge response," *Journal of Bridge Engineering*, Vol. 10, No. 3, pp. 272-280 (2005).
7. Ochsendorf, J. A. and Billington, D. P., "Self-anchored suspension bridges," *Journal of Bridge Engineering*, ASCE, Vol. 4, No. 3, pp. 151-156 (1999).
8. Yang, M. G., Hu, J. H., and Chen, Z. Q., "Seismic response analysis of self-anchored suspension bridge with single-tower," *Journal Centeral South University*, Vol. 36, No. 1, pp. 133-137 (2005).